Desalination and Water Treatment
www.deswater.com
doi: 10.1080/19443994.2013.860631

53 (2015) 2249–2259
February

Taylor & Francis
Taylor & Francis Group

Optimization, kinetics, equilibrium, and thermodynamic investigation of cationic dye adsorption on the fish bone

Alireza Ebrahimi, Elmira Pajootan, Mokhtar Arami*, Hajir Bahrami

Textile Engineering Department, Amirkabir University of Technology, 424 Hafez Ave 15875-4413, Tehran, Iran
Tel. +982164542614; Fax: +98 2166400245; email: arami@aut.ac.ir

Received 1 September 2013; Accepted 19 October 2013

ABSTRACT

The present study evaluates the thermodynamic, kinetic, and isotherm parameters of the adsorption of two cationic dyes as well as the optimization of their removal process using fish bone as the adsorbent. The determination of isoelectric pH (pH_{ZPC}) of the adsorbent demonstrated that the surface of the fish bone was negatively charged at high pH values, which could adsorb cationic dye molecules. The Langmuir, Freundlich, and Tempkin adsorption isotherms were investigated and the results showed that the removal of both dyes followed Tempkin isotherm. Adsorption kinetic studies indicated that the dye removal conformed to pseudo-second-order kinetic model; and calculation of the thermodynamic parameters revealed that the adsorption process was spontaneous ($\Delta G < 0$) and endothermic ($\Delta H > 0$). Also, the response surface methodology was employed for the design of experiments in binary systems using the mixture of both dyes; and the effect of operating parameters (pH, initial dye concentration, adsorbent dosage, and time) was investigated and the removal process was optimized. Eventually, the results indicated that the fish bone can be used as a proper adsorbent for the removal of cationic dyes from multi-component colored wastewaters.

Keywords: Fish bone; Cationic dye; Isotherm; Kinetic; Thermodynamic; Binary system; Response surface methodology.

1. Introduction

The existence of organic dyes in wastewater streams reduces the penetration of sunlight, consumes the dissolved oxygen, and has unpleasant influences on the organic systems. The textile industry uses synthetic dyes extensively and about 15% of dyes during textile processes appears in the wastewaters which must be treated before being discharged to the environment [1–3]. The synthetic dyes are extremely hazardous, toxic, and mutagenic in nature, and in addition, their existence in water streams and their contact with human body can result in irritation, itching, scaling, etc. The complex, persistent, and non-biodegradable structures of these molecules demand their indispensible removal from effluents [4,5].

Among various treatment methods such as coagulation/flocculation, biological, membrane separation, etc. removal of dyes by adsorption technique is of great importance due to the high quality of the treated effluents, simple design, and adsorbents availability [6–8]. Activated carbon (AC) has been one of the

*Corresponding author.

most employed adsorbent in recent years because of its large surface area and high removal efficiency, but the major problem of AC is the expense of its production [7,9,10]. At present the investigations are being focused on finding low cost and effective adsorbents for the efficient removal of pollutants from various wastewaters [11–16]. One of these economic and eco-friendly alternatives for the conventional adsorbents is animal bones like fish bone as an industrial by-product. Calcium ions on the surface of the fish bone make the ion exchange possible for this adsorbent [17–19].

The main objective of the present research is to prepare fish bone adsorbent to study its capability for the removal of cationic dyes from textile wastewaters which according to an eco-toxicological study on cationic dyes, over 18% of 200 dyes tested, showed significant inhibition of the respiration rate of the biomass [20]. Therefore, as the model dyes, C.I. Basic Blue 41 and C.I. Basic Yellow 28 which are among the most commonly used dyestuffs to dye polyacrylonitrile [21], have been chosen for the adsorption studies. In our previous study, the surface characterization of the fish bone was investigated using Fourier transform infrared (FTIR) and scanning electron microscopy (SEM). In the present study, the isoelectric point of the adsorbent was surveyed to determine the surface charge of the fish bone at different media to evaluate the adsorbent capability at various pH values.

Also, adsorption isotherms as a suitable tool to predict and explain the adsorption system and to describe the interaction between the adsorbate and adsorbent were investigated [22,23]. The adsorption data for both dyes were studied using Langmuir, Freundlich, and Tempkin isotherm models. Thermodynamic parameters of fish bone were also calculated to determine the spontaneous and exo/endothermic nature of the adsorption process [22,24]. The adsorption data were modeled adopting the pseudo-first and pseudo-second-order kinetic equation models [25]. Finally, in order to study the fish bone capability in multi-component dye solutions, the dye removal efficiency of binary systems containing the combination of both basic dyes was investigated using response surface methodology (RSM) [26]. RSM as a very useful statistical tool has been employed in many researching including water and wastewater treatment [27–30]. In this regard, herein, the adsorption process in binary systems was optimized and the optimal removal efficiency predicted by response optimizer was compared with the performed experiments at the predicted conditions.

2. Materials and methods

The fish bone was purchased from the wastes of the tuna canning factory in the city of Rasht-Iran. According to our previous study [19], the first step for the preparation of the adsorbent was the separation of fish bones from meat and washing them with distilled water at 100˚C for several times. Then, the fish bones were washed with hot distilled water and dried for 40 min at 150˚C. The dried fish bones were milled with a mortar to particle sizes of 250 μm.

C.I. Basic Yellow 28-BY28 (C.I. Constitution No. 48054, molecular weight = 433.52 g/mol and λ_{max} = 438 nm) and C.I. Basic Blue 41-BB41 (C.I. Constitution No. 11105, molecular weight = 482.57 g/mol and λ_{max} = 606 nm) purchased from CIBA were used as synthetic dyes. Table 1 represents the chemical structures of both dyes which were stable at the pH range (2–11) studied in this research. Two-hundred milliliters of synthetic dye solutions were prepared by diluting 1,000 mg/L of stock solution with distilled water. NaOH (Merck) and H_2SO_4 (Merck) were used for pH adjustment of the solutions. A magnetic stirrer was used for mixing the solutions at 200 rpm. The samples were taken from the solution and then centrifuged at 4,000 rpm for 10 min. The absorbance of the samples was measured at their maximum wavelength (λ_{max}) by UNICO 2100 Spectrophotometer.

Thermodynamic study was carried out at 298, 308, 318, and 328 *K* with the dye concentration of 50 mg/L at pH 11 and adsorbent dosage of 2.5 g/L. The adsorption isotherms were investigated at pH 11 and adsorbent dosage of 2.5 g/L, at temperature range of 298 to 328 *K*, and initial dye concentrations of 50, 100, and 150 mg/L. To study the kinetics of adsorption

Table 1
Dye structures

C.I. Basic Blue 41

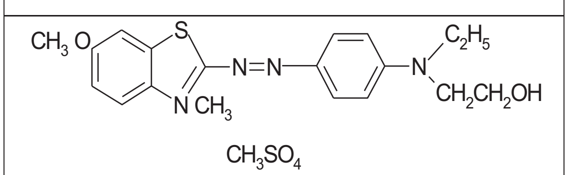

C.I. Basic Yellow 28

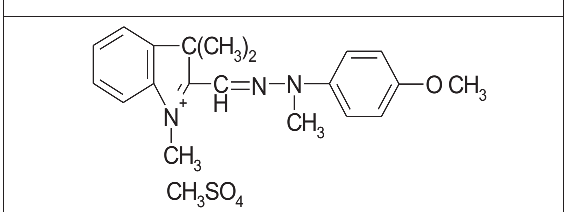

process using the fish bone, experiments were carried out in 200 mL dye solution with different initial concentrations of 50, 100, and 150 mg/L, adsorbent dosage of 2.5 g/L, and pH of 11 at room temperature.

3. Results and discussion

3.1. Characterization of the fish bone

As investigated in our previous study [19], the Fourier transform infrared (FTIR) analysis (Nicolet FTIR instrument) in the range of 500–4,000 cm^{-1} determined the functional groups of the fish bone adsorbent. The peaks related to the symmetric bending of C–H, stretching bonds of O–H, C=O, and C–O appeared at 2924.59 and 2859.83, 3431.64, 1741.91, and 1034.67 cm^{-1}, respectively, and the carbonyl, carboxyl, and hydroxyl functional groups were found to be responsible for the adsorption of cationic dye molecules. Also, the surface morphology of the fish bone investigated by SEM showed that the fish bone had a relatively porous surface with heterogeneous holes, which makes it a suitable adsorbent with large surface area for the adsorption of dyes.

In order to determine the isoelectric pH (pH_{ZPC}) of the adsorbent, 1.0 g of fish bone was added to 50 mL KNO_3 solutions (0.01 M). The initial pH of the solutions was adjusted from 2 to 11. The solutions were stirred for 24 h and the final pH was recorded. The final pH vs. the initial pH is plotted in Fig. 1. The pH in which the value of (pH_i–pH_f) equals zero is known as the pH_{ZPC} being equal to 7 in this study. This means that the surface of the fish bone at pH > 7 is negatively charged and at pH values lower than 7 contains positive charges. Therefore, the cationic dyes can be adsorbed on the surface of the adsorbent at high pH values.

3.2. Effect of operating parameters

The experiments were carried out by varying pH of the solution (2, 7, and 11) while keeping other factors at a specified value. After the determination of optimum pH value, the effect of adsorbent dosage (0.5, 2.5, and 5 g/L), and initial dye concentration (50, 100, and 200 mg/L) were investigated.

3.2.1. The effect of pH

The effect of initial pH on the removal efficiency and adsorption capacity of BB41 and BY28 uptake by the fish bone after 60 min was investigated. When the pH of solution was increased from 2 to 11, the dye removal also increased from 28.22% ($q_t = 11.28$ mg/g) to 93.41% ($q_t = 37.33$ mg/g) and from 29.10% ($q_t =$ 11.63 mg/g) to 29.10% ($q_t = 33.69$ mg/g) for BB41 and BY28, respectively. At high pH values (pH > $pH_{ZPC} =$ 7), the surface of the fish bone is negatively charged and the cationic dye molecules are adsorbed on the surface of the fish bone by electrostatic attraction forces. On the other hand, at low pH values (pH < 7) the dye removal efficiency decreased due to the repulsion between the positively charged functional groups of the fish bone and the cationic dye molecules [31–33].

3.2.2. The effect of adsorbent dosage

The effect of adsorbent dosage on the dye removal efficiency and adsorption capacity of fish bone was investigated by varying the adsorbent dosage from 0.5 to 5 g/L. According to the results presented in Fig. 2, by increasing the adsorbent dosage, the removal percentage increases. It was found that when the adsor-

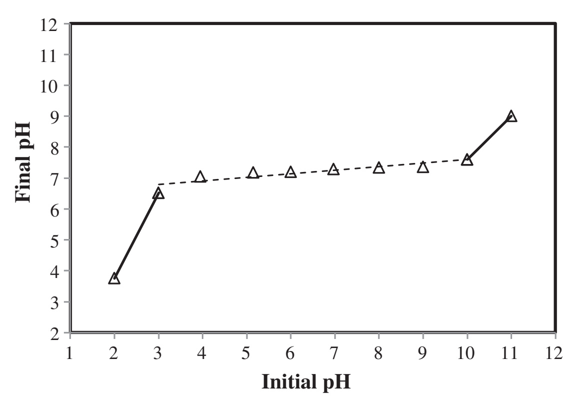

Fig. 1. pH_{ZPC} plot of the fish bone.

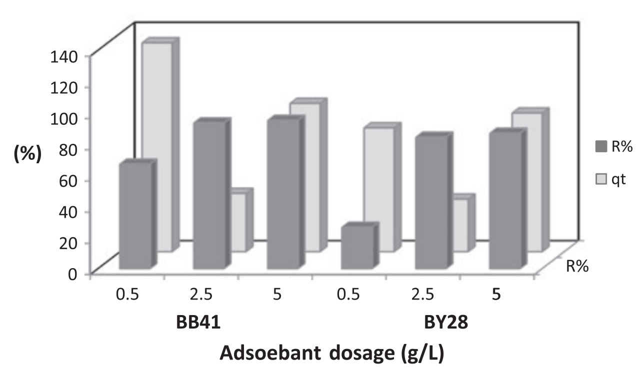

Fig. 2. The effect of adsorbent dosage on dye removal % and q_t (mg/g) of BY28 and BB41. Initial dye concentration: 100 mg/L, pH 11, and time: 60 min.

bent dosage was increased from 0.5 to 2.5 g/L, the dye removal efficiency increased from about 67 to 93.5% for both dyes. By increasing the amount of adsorbent up to 5.0 g/l, the dye removal efficiency will increase to 95.06%. Also, it has been calculated that with increasing the adsorbent dosage, the q_0 (the amount of dye adsorbed per unit mass of adsorbent at equilibrium) will decrease from 133.9 to 19.01 mg/g; hence, 2.5 g/L has been chosen for the optimum amount of adsorbent dosage. Increasing the amount of adsorbent, results in more adsorption sites and available sorption surface to interact with dye molecules, that leads to the higher dye removal efficiency [34,35].

3.2.3. The effect of initial dye concentration and kinetic studies

The influence of varying the initial dye concentration from 50 to 200 mg/L on the adsorption performance was investigated and the results are shown in Fig. 3. Increasing the dye concentration has decreased the dye removal (%) and the equilibrium adsorption capacity for both BB41 and BY28. At lower dye concentrations, more adsorption sites are free and available for the adsorption of dye molecules, but increasing the initial dye concentration leads to the less available sites for dye molecules to be adsorbed, and as a result the dye removal decreases [36–38].

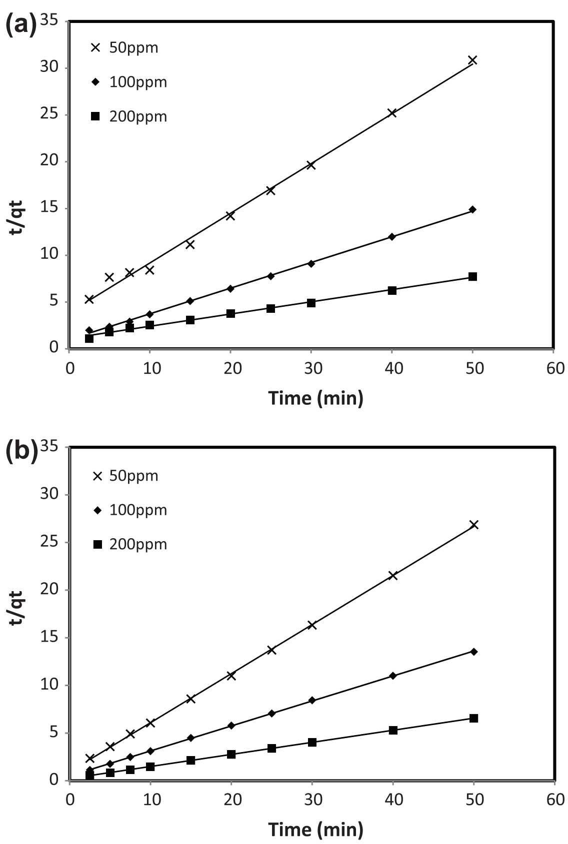

Fig. 3. The effect of initial dye concentration on dye removal (%) and pseudo-second-order kinetic; (a) BY28, (b) BB41. pH 11 and adsorbent dosage: 2.5 g/L.

In order to investigate the adsorption dynamics, the kinetics data were evaluated. In this regard, two kinetic models; pseudo-first and pseudo-second-order were used to describe the adsorption kinetics [22,39–41]. Pseudo-first-order equation is generally written as:

$$\frac{dq_t}{dt} = k_1(q_e - q_t) \tag{1}$$

where q_e and k_1 are the amount of dye adsorbed at equilibrium (mg/g) and the equilibrium rate constant of pseudo-first-order kinetics (1/min), respectively. Integrating and applying the conditions, $q_t = 0$ at $t = 0$ and $q_t = q_t$ at $t = t$, will lead to the Eq. (2) [23]:

$$\log(q_e - q_t) = \log(q_e) - \left(\frac{k_1}{2.303}\right)t \tag{2}$$

The data obtained by the adsorption process were also applied to the pseudo-second-order kinetic which is represented as follows [42]:

$$\frac{dq_t}{dt} = k_2(q_e - q_t) \tag{3}$$

where k_2 is the equilibrium rate constant of pseudo-second-order model (g/(mg.min)). The integration of Eq. (3) can be expressed as [43]:

$$\frac{t}{q_t} = \frac{1}{k_2 q_e^2} + \left(\frac{1}{q_e}\right)t \tag{4}$$

The values of k_1, k_2, R_1^2 (correlation coefficient for pseudo-first-order model) and R_2^2 (correlation coefficient for pseudo-second-order model) have been calculated by varying the initial dye concentration, pH, adsorbent dosage, and temperature (data not shown). According to Fig. 3, the adsorption kinetics of both BB41 and BY28 followed pseudo-second-order model ($R_2^2 > 0.97$), but pseudo-first-order model did not fit well to the obtained results.

3.3. Adsorption Isotherms

The determination of the most appropriate correlation for the equilibrium curve is very important

Table 2
Isotherm parameters for the adsorption of BB41 and BY28 onto fish bone

		Tempkin			Langmuir			Freundlich		
		R_1^2	B_T	A_T	R_2^2	Q_0	B	${R_3}^2$	K_f	n
298K	BB41	0.999	44.568	0.0046	0.989	30.487	0.032	0.997	1,547.04	1.238
	BY28	0.997	51.384	0.0045	0.954	22.570	0.023	0.988	5,910.17	0.922
308K	BB41	0.999	49.991	0.0046	0.987	31.446	0.037	0.997	1,383.25	1.281
	BY28	0.997	43.715	0.0044	0.956	24.096	0.024	0.989	4,491.59	0.979
318K	BB41	0.000	43.630	0.0045	0.986	31.546	0.037	0.997	1,386.36	1.285
	BY28	0.997	50.378	0.0045	0.953	23.697	0.023	0.988	4,842.84	0.963
328K	BB41	0.999	44.611	0.0047	0.992	30.487	0.036	0.998	1,552.04	1.237
	BY28	0.999	50.682	0.0045	0.980	23.809	0.023	0.995	4,910.21	0.962

for the optimization of an adsorption system to remove dyes from solutions. Several isotherm models have been used in the literatures. In this study, the adsorption data of basic dyes by the fish bone were analyzed using Langmuir, Freundlich, and Tempkin isotherm models. The Langmuir model as the most frequently employed isotherm describing the monolayer adsorption of dye molecules on a homogeneous surface with a finite number of identical sites is given by Eq. (5) [4]:

$$q_e = \frac{Q_0 K_L C_e}{1 + K_L C_e} \tag{5}$$

where C_e, Q_0, and K_L are the equilibrium concentration of the adsorbate (mg/L), maximum adsorption capacity (mg/g), and Langmuir constant (L/mg), respectively.

The Freundlich isotherm assumes a heterogeneous surface with a nonuniform distribution of heat of adsorption over the surface and can be expressed by:

$$q_e = K_F C_e^{\frac{1}{n}} \tag{6}$$

where K_F is the adsorption capacity at unit concentration and $1/n$ is adsorption intensity. $1/n$ values indicate the type of isotherm to be irreversible ($1/n = 0$), favorable ($0 < 1/n < 1$) and unfavorable ($1/n > 1$). Eq. (7) can be rearranged to the linear form as follows:

$$\log q_e = \log K_F + \left(\frac{1}{n}\right) \log C_e \tag{7}$$

The Tempkin isotherm assumes that the heat of adsorption of all the molecules in the layer decreases

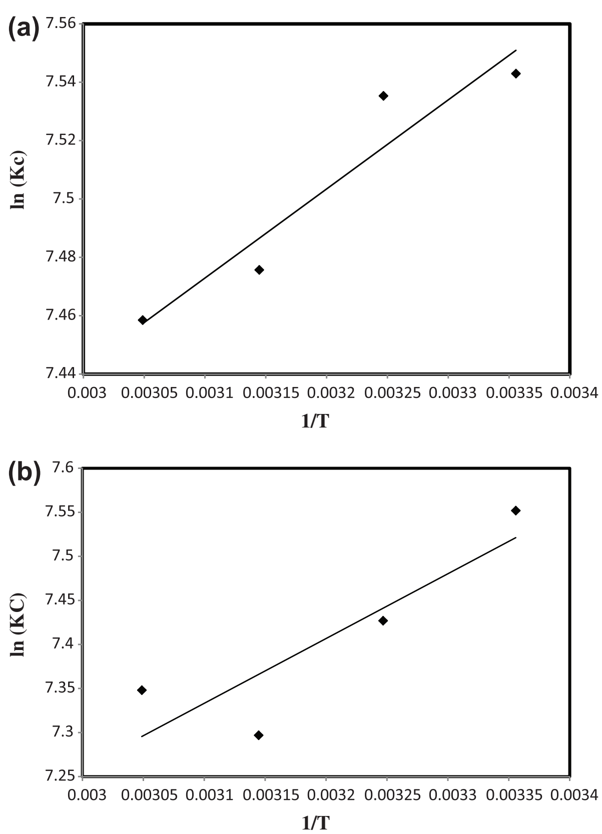

Fig. 4. Thermodynamic plots of the adsorption of (a) BY28, (b) BB41 onto the fish bone. pH 11, initial dye concentration: 50 mg/L, and adsorbent dosage: 2.5 g/L.

Table 3
Thermodynamic parameters for the adsorption of BB41 and BY28 onto fish bone

Dye	Δs	ΔH	ΔG (298K)	ΔG (308K)	ΔG (318K)	ΔG (328K)
BB41	63.15	0.62	−18.81	−19.44	−20.06	−20.70
BY28	63.03	0.26	−18.78	−19.41	−20.04	−20.67

linearly with coverage due to the adsorbent–adsorbate interactions and that the adsorption is characterized by a uniform distribution of binding energies, up to some maximum level. The nonlinear and linear forms of the Tempkin isotherm are given as Eqs. (8) and (9), respectively:

$$q_e = \frac{RT}{b} \ln(K_T C_e) \tag{8}$$

$$q_e = B_1 \ln K_T + B_1 \ln C_e \tag{9}$$

where

$$B_1 = \frac{RT}{b} \tag{10}$$

where T and R are the absolute temperature (K) and the universal gas constant (8.314 J/(mol K)), respectively. B_1 and K_T are the Tempkin constant and b is related to the heat of adsorption [44,45].

To study the applicability of the mentioned isotherms for dye adsorption onto fish bone at different temperatures, linear plots of C_e/q_e against C_e, $\log q_e$ vs. $\log C_e$ and q_e vs. $\ln C_e$ were plotted, respectively, and the values of Q_0, K_L, K_F, $1/n$, B_T, A_T, and R^2 (correlation coefficient values of all isotherms models) are shown in Table 2. The correlation coefficient values illustrate that the dye removal does not follow the Langmuir and Freundlich isotherms. The calculated correlation coefficients (R^2) for Tempkin isotherm model indicate that the dye removal isotherm can be approximated by the Tempkin model. This means that the heat of adsorption of all the molecules in the layer decreases linearly with coverage due to the interactions of adsorbent and adsorbate [33,46].

3.4. Thermodynamic parameters

The thermodynamic parameters of the adsorption process can be determined from the experimental data using the following equations:

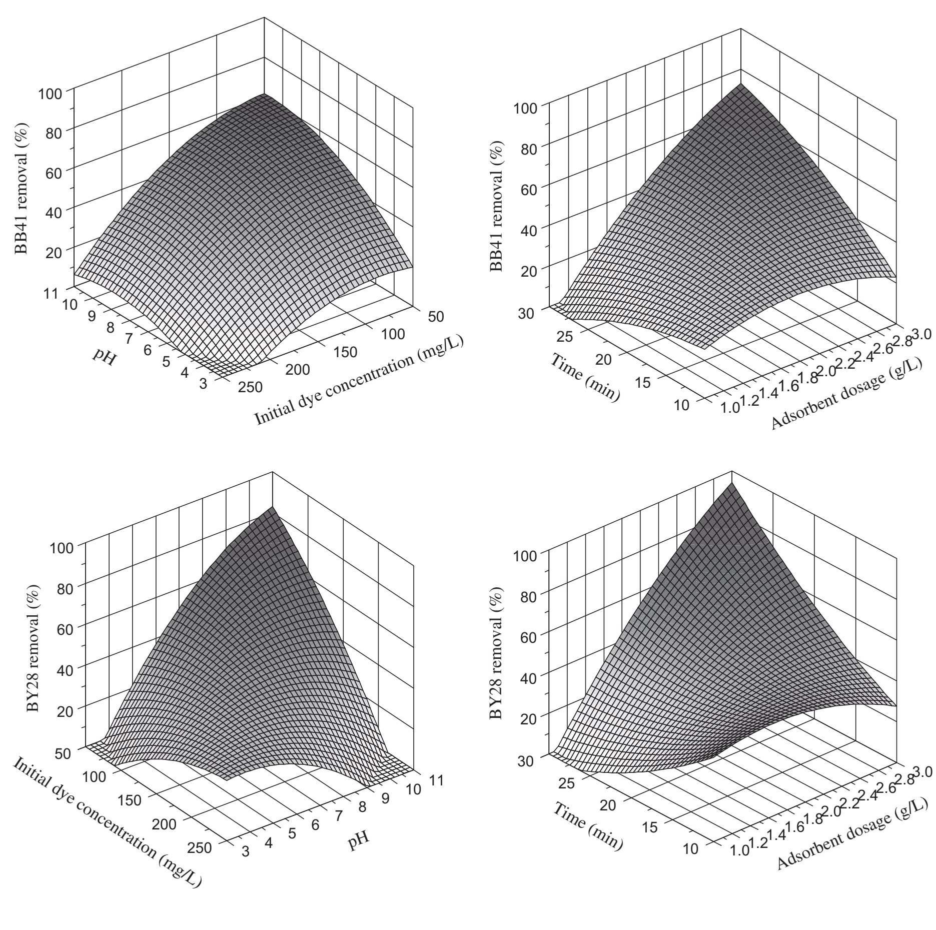

Fig. 5. 3D surface plots for dye removal using fishbone.

Table 4
CCD matrix for BB41 and BY28 removal in binary system

	pH	Initial dye conc. (mg/L)	Adsorbent dosage (g/L)	Time (min)	BB41 removal (%)	Pre. BB41 removal (%)	BY28 removal (%)	Pre. BY28 removal (%)
1	9	200	1.5	25	35.43	38.40	41.68	37.98
2	7	150	3.0	20	54.93	46.32	58.56	50.54
3	9	100	2.5	25	39.91	48.55	45.78	54.37
4	5	100	1.5	15	28.76	31.12	36.09	34.35
5	9	200	2.5	25	52.18	55.27	56.58	60.70
6	7	150	2.0	10	28.91	25.73	47.27	39.70
7	7	150	2.0	20	44.86	44.47	53.98	50.45
8	7	150	2.0	20	43.81	44.16	54.66	50.45
9	5	100	2.5	20	50.42	46.01	56.95	45.69
10	9	100	2.5	15	19.07	35.11	35.59	43.72
11	5	100	1.5	25	24.41	26.47	26.96	30.15
12	5	200	2.5	25	31.82	33.05	40.84	39.22
13	9	100	1.5	15	37.92	36.01	33.78	36.63
14	7	150	2.0	30	46.60	43.90	55.25	56.41
15	7	150	2.0	20	43.16	45.38	48.16	50.45
16	5	100	2.5	15	45.42	43.99	35.08	45.63
17	7	150	2.0	20	44.58	44.16	48.77	50.45
18	7	150	2.0	20	43.96	42.83	49.04	50.45
19	7	150	2.0	20	44.21	44.55	47.56	50.45
20	7	150	1.0	20	12.75	16.59	12.12	16.54
21	7	250	2.0	20	11.25	16.70	19.86	24.25
22	9	200	2.5	15	35.19	32.46	41.76	39.79
23	7	50	2.0	20	53.65	43.42	54.01	46.02
24	5	200	2.5	15	22.73	24.30	26.94	30.05
25	7	150	2.0	20	43.46	42.98	48.16	50.45
26	5	200	1.5	15	7.00	-2.32	13.62	6.25
27	9	100	1.5	25	41.55	45.43	44.90	44.17
28	9	200	1.5	15	11.96	19.61	12.17	20.18
29	11	150	2.0	20	61.96	45.53	51.00	40.16
30	3	150	2.0	20	6.75	18.41	9.16	16.40
31	5	200	1.5	25	13.00	2.40	18.06	12.31

$$\ln K_c = \frac{\Delta S}{R} - \frac{\Delta H}{RT} \tag{11}$$

$$\Delta G = \Delta H - T\,\Delta S \tag{12}$$

$$K_c = \frac{q_e}{C_e} \tag{13}$$

where ΔS, ΔH, and ΔG are the changes of entropy, enthalpy, and Gibbs free energy; and K_c, T, and R are the distribution coefficient for the adsorption, temperature (K), and gas constant (J/(mol K)), respectively [47–49]. The values of ΔH and ΔS were calculated from the slopes and intercepts obtained from the plots of $\ln K_c$ vs. $1/T$ (Fig. 4).

The ΔH, ΔS, and ΔG values at different temperatures for the adsorption of basic dyes are given in Table 3. The data indicate that the nature of adsorption process is spontaneous and thermodynamically able to be carried out at room temperature due to the negative values of ΔG. The positive ΔS values point out that during the adsorption of dyes onto the fish bone, the randomness at the solid–solution interface increases. The results also showed that at higher temperatures the amount of adsorbed dye increased, which indicated that the adsorption of basic dyes onto the fish bone was an endothermic process ($\Delta H > 0$). These results may be explained by the increase of the mobility of large dye molecules depending on the temperature and the subsequent interacting of these molecules with adsorption sites. Moreover, the alteration of temperature up to 328 K may induce a swelling effect within the internal structure of the fish bone enabling the same molecules to penetrate further [50–52].

3.5. RSM for binary system and process optimization

Real wastewaters often include more than one component and the study of possible dye removal from wastewaters containing the mixture of dyes like binary systems can be very useful for the treatment of real industrial wastewaters. Therefore, in this paper, the dye removal of the mentioned cationic dyes in binary system was also studied. RSM is a statistical alternative to the conventional method that is suitable for modeling and obtaining optimum conditions for the considered response [53–55]. According to the results from classical experiments, a central composite design (CCD) was used as an efficient design tool for fitting the second-order models. Four factors with five levels including pH (X_1), initial dye concentration (X_2), adsorbent dosage (X_3), and reaction time (X_4) were considered as input variables. The dye removal efficiencies resulted from 31 adsorption processes are presented in Table 4. The removal of BB41 and BY28 has been calculated separately for each dye at their maximum wavelengths [56].

According to Eq. (14), the dye removal efficiency (Y_i: response variable) is related to the input factors using the coefficients of the polynomial model:

$$Y_i = a_0 + \sum_{i=1}^{n} a_i x_i + \sum_{i=1}^{n} a_{ii} x_i^2 + \sum_{i=1}^{n-1} \sum_{j=i+1}^{n} a_{ij} x_i x_j \quad (14)$$

where a_0, a_i, a_i, and a_{ij} are constant coefficient, regression coefficients for linear effects, the quadratic coefficients, and interaction coefficients, respectively; while, x_i and x_j are the coded values of input factors [57]. The coefficients and P values obtained from the CCD experiments results are represented in Table 5.

It should be mentioned that only the significant factors (P value ≤ 0.05) will be presented in Eq. (16). According to the results, all independent parameters for both dyes are significant.

Table 5
The obtained coefficients and P values for BB41 and BY28 removal in binary system

	BB41 removal		BY28 removal	
Terms	Coef	P	Coef	P
Constant	44.158	0	50.4481	0
pH	6.78	0.002	5.9386	0.003
Dye con.	−6.679	0.003	−5.4433	0.005
Ads.	7.434	0.001	8.4999	0
Time	4.542	0.032	4.1777	0.027
pH × pH	−3.047	0.092	−5.5417	0.002
Dye con. × dye con.	−3.524	0.055	−3.8278	0.023
Ads. × ads.	−3.175	0.08	−4.2271	0.013
Time × time	−2.335	0.189	−0.5988	0.698
pH × dye con.	4.259	0.082	2.9122	0.174
pH × ads.	−3.443	0.153	−1.047	0.616
pH × time	3.517	0.163	2.9354	0.19
Dye con. × ads.	3.437	0.154	3.1284	0.146
Dye con. × time	2.343	0.345	2.5648	0.249
Ads. × time	1.006	0.681	0.7763	0.722

The ANOVA analysis of the model is represented in Table 6. A fair coefficient of determination (R^2: 81.56% for BB41 and R^2: 84.70% for BY28) and no lack of fit for the model indicated that the model equation resulted from RSM can be used to describe the adsorption process using the fish bone, which also validates the statistical significance of the model [58].

Here, some of the three-dimensional plots are presented in Fig. 5 to investigate the simultaneous interaction of two factors on dye removal efficiency. According to Fig. 5, the statistical results for binary systems and classical results for single systems are in excellent agreement. 3D surface plots in Fig. 5 shows the effect of operating parameters on the color removal efficiency. According to these plots, increasing the pH value and decreasing the initial dye concentration simultaneously will increase both BB41 and

Table 6
ANOVA for dye removal using fish bone

	BB41 removal						BY28 removal					
Source	DF	Seq SS	Adj SS	Adj MS	F	P	DF	Seq SS	Adj SS	Adj MS	F	P
Regression	14	5,833.45	5,833.45	416.67	5.06	0.001	14	5,800.67	5,800.67	414.33	6.33	0
Linear	4	4,052.53	3,858.51	964.63	11.71	0	4	3,777.72	3,575.23	893.81	13.65	0
Square	4	796.34	801.81	200.45	2.43	0.09	4	1,479.52	1,507.36	376.84	5.75	0.005
Interaction	6	984.58	984.58	164.1	1.99	0.127	6	543.43	543.43	90.57	1.38	0.28
Residual error	16	1,318.59	1,318.59	82.41	–	–	16	1,047.86	1,047.86	65.49	–	–
Lack-of-fit	10	1,316.45	1,316.45	131.65	370.32	0	10	995.16	995.16	99.52	11.33	0.004
Pure error	6	2.13	2.13	0.36	–	–	6	52.71	52.71	8.78	–	–
Total	30	7,152.03	–	–	–	–	30	6,848.53	–	–	–	–

BY28 removal efficiencies due to the existence of more negative charges on the surface of the adsorbent and a fewer number of dye molecules in the solution which could move toward the adsorbent and be removed from the solution. Moreover, increasing the adsorbent dosage and the adsorption process time will also increase the dye removal (%).

The Response Optimizer (Minitab software) was applied to optimize the parameters affecting the adsorption process to reach 70 and 65% of dye removal efficiency for BY28 and BB41, respectively. According to our obtained results, the adsorption capacity of the fish bone was higher for BY28 probably due to the lower molecular weight and less hydrophilic group in its structure, which make the dye molecules to access the adsorption sites of the fish bone more easily. As a result, the value of the removal percentage considered for BB41 was lower. The optimum values predicted by the software were pH: 10.27, initial dye concentration: 213.63 mg/L, adsorbent dosage: 2.69 g/L, and the time of 30 min for the adsorption process with the composite desirability of 0.86. To evaluate the adsorption process applying the obtained conditions, three experiments were performed. The calculated average values for dye removal efficiencies were 69.32 and 64.21% for BY28 and BB41, respectively, which are in a satisfactory agreement with the predicted values.

4. Conclusion

The present study investigated the use of the fish bone as an adsorbent for the removal of cationic dyes from colored textile wastewaters. The determination of isoelectric pH (pH_{ZPC}) indicated that the fish bone was negatively charged at high pH values, which seems to be suitable for the removal of cationic dyes (BB41 and BY28) from colored solutions. Isotherm, kinetic, and thermodynamic parameters of the adsorption process were studied. The resulted data of the adsorption process have followed Tempkin isotherm. Also, the second-order kinetic model (high R^2 values) was best fitted to the obtained results. The adsorption procedure was found to be spontaneous and endothermic according to the negative and positive values of ΔG and ΔH, respectively. In order to evaluate the fish bone more effectively, the binary systems containing the mixture of both cationic dyes were studied using RSM. The effect of operating parameters including initial dye concentration, pH, time, and adsorbent dosage was evaluated by RSM and all of these four factors were significant to the model. By using this method, both the effect of operating parameters on the adsorption process and their relation to the dye removal efficiency was studied as well as the process optimization. The most obvious conclusion from our results was that the effect of different operating parameters on the performance of adsorption process for the single system was the same as the binary system and the dye removal efficiency values were too close to each other. Altogether, the mathematical model can serve as a management tool for wastewater treatment and it can also be concluded that adsorption using the low-cost fish bone is a successful and promising process with high efficiencies for the removal of cationic dyes from wastewaters containing multiple component.

References

[1] S. Elemen, E.P. Akçakoca Kumbasar, S. Yapar, Modeling the adsorption of textile dye on organoclay using an artificial neural network, Dyes Pigments 95 (2012) 102–111.
[2] M. Anbia, S. Salehi, Removal of acid dyes from aqueous media by adsorption onto amino-functionalized nanoporous silica SBA-3, Dyes Pigments 94 (2012) 1–9.
[3] S. Chowdhury, R. Mishra, P. Saha, P. Kushwaha, Adsorption thermodynamics, kinetics and isosteric heat of adsorption of malachite green onto chemically modified rice husk, Desalination 265 (2011) 159–168.
[4] M. Asgher, H.N. Bhatti, Mechanistic and kinetic evaluation of biosorption of reactive azo dyes by free, immobilized and chemically treated Citrus sinensis waste biomass, Ecol. Eng. 36 (2010) 1660–1660.
[5] Y. Safa, H.N. Bhatti, Kinetic and thermodynamic modeling for the removal of Direct Red-31 and Direct Orange-26 dyes from aqueous solutions by rice husk, Desalination 272 (2011) 313–322.
[6] N.M. Mahmoodi, B. Hayati, M. Arami, C. Lan, Adsorption of textile dyes on Pine Cone from colored wastewater: Kinetic, equilibrium and thermodynamic studies, Desalination 268 (2011) 117–125.
[7] B. Cheknane, F. Zermane, M. Baudu, O. Bouras, J.P. Basly, Sorption of basic dyes onto granulated pillared clays: Thermodynamic and kinetic studies, J. Colloid Interface Sci. 381 (2012) 158–163.
[8] A. Mittal, J. Mittal, L. Kurup, Adsorption isotherms, kinetics and column operations for the removal of hazardous dye, Tartrazine from aqueous solutions using waste materials—Bottom Ash and De-Oiled Soya, as adsorbents, J. Hazard. Mater. 136 (2006) 567–578.
[9] C. Shen, Y. Shen, Y. Wen, H. Wang, W. Liu, Fast and highly efficient removal of dyes under alkaline conditions using magnetic chitosan-Fe(III) hydrogel, Water Res. 45 (2011) 5200–5210.
[10] N.M. Mahmoodi, R. Salehi, M. Arami, Binary system dye removal from colored textile wastewater using activated carbon: Kinetic and isotherm studies, Desalination 272 (2011) 187–195.
[11] D. Mohan, S. Rajput, V.K. Singh, P.H. Steele, C.U. Pittman Jr., Modeling and evaluation of chromium remediation from water using low cost bio-char, a green adsorbent, J. Hazard. Mater. 188 (2011) 319–333.

[12] S.D. Khattri, M.K. Singh, Removal of malachite green from dye wastewater using neem sawdust by adsorption, J. Hazard. Mater. 167 (2009) 1089–1094.
[13] M.A.K.M. Hanafiah, W.S.W. Ngah, S.H. Zolkafly, L.C. Teong, Z.A.A. Majid, Acid Blue 25 adsorption on base treated Shorea dasyphylla sawdust: Kinetic, isotherm, thermodynamic and spectroscopic analysis, J. Environ. Sci. 24 (2012) 261–268.
[14] S. Noreen, H.N. Bhatti, S. Nausheen, S. Sadaf, M. Ashfaq, Batch and fixed bed adsorption study for the removal of Drimarine Black CL-B dye from aqueous solution using a lignocellulosic waste: A cost affective adsorbent, Ind. Crops Prod. 50 (2013) 568–579.
[15] A. Mittal, J. Mittal, L. Kurup, Utilization of hen feathers for the adsorption of indigo carmine from simulated effluents, J. Environ. Prot. Sci. 1 (2007) 92–100.
[16] S. Sadaf, H.N. Bhatti, I. Bibi, Efficient removal of disperse dye by mixed culture of ganoderma lucidum and coriolus versicolor, Pak. J. Agri. Sci. (2013) 261–266.
[17] B. Kizilkaya, A.A. Tekinay, Y. Dilgin, Adsorption and removal of Cu (II) ions from aqueous solution using pretreated fish bones, Desalination 264 (2010) 37–47.
[18] H.K. Lim, T.T. Teng, M.H. Ibrahim, A. Ahmad, H.T. Chee, Adsorption and removal of zinc (II) from aqueous solution using powdered fish bones, APCBEE Procedia 1 (2012) 96–102.
[19] A. Ebrahimi, M. Arami, H. Bahrami, E. Pajootan, Fish bone as a low-cost adsorbent for dye removal from wastewater: response surface methodology and classical method, Environ. Model. Assess 18(16) (2013) 1–10.
[20] P. Cooper, Color in dyehouse effluent, Society of Dyers and Colourists, on behalf of the Dyers' Company Publications Trust, Bradford, 1995.
[21] M.A. Méndez, G.R. Tovar, M.M. Dávila, O. Ornelas, M.P. Elizalde, Degradation of reactive Black 5 and basic Yellow 28 on metallic-polymer composites, Portugaliae Electrochim. Acta 26 (2008) 89–100.
[22] L. Wang, Application of activated carbon derived from 'waste' bamboo culms for the adsorption of azo disperse dye: Kinetic, equilibrium and thermodynamic studies, J. Environ. Manage. 102 (2012) 79–87.
[23] M. Asgher, H.N. Bhatti, Removal of reactive blue 19 and reactive blue 49 textile dyes by citrus waste biomass from aqueous solution: Equilibrium and kinetic study, Canadian J. Chem. Eng. 90 (2012) 412–419.
[24] V.M. Vučurović, R.N. Razmovski, M.N. Tekić, Methylene blue (cationic dye) adsorption onto sugar beet pulp: Equilibrium isotherm and kinetic studies, J. Taiwan Inst. Chem. E. 43 (2012) 108–111.
[25] M.M.F. Silva, M.M. Oliveira, M.C. Avelino, M.G. Fonseca, R.K.S. Almeida, E.C. Silva Filho, Adsorption of an industrial anionic dye by modified-KSF-montmorillonite: Evaluation of the kinetic, thermodynamic and equilibrium data, Chem. Eng. J. 203 (2012) 259–268.
[26] V.K. Sharma, S. Solanki, Topological investigations of binary mixtures containing 1-ethyl-3-methylimidazolium tetrafluoroborate and anilines, J. Mol. Liq. 177 (2013) 133–144.
[27] M.H. Muhamad, S.R. Sheikh Abdullah, A.B. Mohamad, R. Abdul Rahman, A.A. Hasan Kadhum, Application of response surface methodology (RSM) for optimisation of COD, NH3–N and 2,4-DCP removal from recycled paper wastewater in a pilot-scale granular activated carbon sequencing batch biofilm reactor (GAC-SBBR), J. Environ. Manage. 121 (2013) 179–190.
[28] Y. Yang, Y. Li, Y.-M. Zhang, D.-W. Liang, Applying hybrid coagulants and polyacrylamide flocculants in the treatment of high-phosphorus hematite flotation wastewater (HHFW): Optimization through response surface methodology, Sep. Purif. Technol. 76 (2010) 72–78.
[29] P.A. Soloman, C. Ahmed Basha, M. Velan, N. Balasubramanian, P. Marimuthu, Augmentation of biodegradability of pulp and paper industry wastewater by electrochemical pre-treatment and optimization by RSM, Sep. Purif. Technol. 69 (2009) 109–117.
[30] E. Yuliwati, A.F. Ismail, W.J. Lau, B.C. Ng, A. Mataram, M.A. Kassim, Effects of process conditions in submerged ultrafiltration for refinery wastewater treatment: Optimization of operating process by response surface methodology, Desalination 287 (2012) 350–361.
[31] I.D. Mall, V.C. Srivastava, N.K. Agarwal, Removal of Orange-G and Methyl Violet dyes by adsorption onto bagasse fly ash—Kinetic study and equilibrium isotherm analyses, Dyes Pigments 69 (2006) 210–223.
[32] C. Kannan, K. Muthuraja, M.R. Devi, Hazardous dyes removal from aqueous solution over mesoporous aluminophosphate with textural porosity by adsorption, J. Hazard. Mater. 244–245 (2013) 10–20.
[33] A. Mittal, V. Thakur, J. Mittal, H. Vardhan, Process development for the removal of hazardous anionic azo dye Congo red from wastewater by using hen feather as potential adsorbent, Desalin. Water Treat. (2013) 1–11.
[34] R. Gong, M. Li, C. Yang, Y. Sun, J. Chen, Removal of cationic dyes from aqueous solution by adsorption on peanut hull, J. Hazard. Mater. 121 (2005) 247–250.
[35] V.K. Garg, R. Gupta, A. Bala Yadav, R. Kumar, Dye removal from aqueous solution by adsorption on treated sawdust, Bioresour. Technol. 89 (2003) 121–124.
[36] A. Mittal, D. Jhare, J. Mittal, Adsorption of hazardous dye Eosin Yellow from aqueous solution onto waste material De-oiled Soya: Isotherm, kinetics and bulk removal, J. Mol. Liq. 179 (2013) 133–140.
[37] M. Constantin, I. Asmarandei, V. Harabagiu, L. Ghimici, P. Ascenzi, G. Fundueanu, Removal of anionic dyes from aqueous solutions by an ion-exchanger based on pullulan microspheres, Carbohydr. Polym. 91 (2013) 74–84.
[38] M. Ajbary, A. Santos, V. Morales-Flórez, L. Esquivias, Removal of basic yellow cationic dye by an aqueous dispersion of Moroccan stevensite, Appl. Clay Sci. 80–81 (2013) 46–51.
[39] M.S.U. Rehman, I. Kim, J.-I. Han, Adsorption of methylene blue dye from aqueous solution by sugar extracted spent rice biomass, Carbohydr. Polym. 90 (2012) 1314–1322.
[40] T.A. Khan, S. Dahiya, I. Ali, Use of kaolinite as adsorbent: Equilibrium, dynamics and thermodynamic studies on the adsorption of Rhodamine B from aqueous solution, Appl. Clay Sci. 69 (2012) 58–66.
[41] N.K. Amin, Removal of direct blue-106 dye from aqueous solution using new activated carbons developed from pomegranate peel: Adsorption equilibrium and kinetics, J. Hazard. Mater. 165 (2009) 52–62.

[42] H. Daraei, A. Mittal, M. Noorisepehr, F. Daraei, Kinetic and equilibrium studies of adsorptive removal of phenol onto eggshell waste, Environ. Sci. Pollut. Res. 20 (2013) 4603–4611.
[43] J.Mittal, D.Jhare, H.Vardhan, A.Mittal, Utilization of bottom ash as a low-cost sorbent for the removal and recovery of a toxic halogen containing dye eosin yellow, Desalin. Water Treat. (2013) 1–12.
[44] G.L. Dotto, J.M. Moura, T.R.S. Cadaval, L.A.A. Pinto, Application of chitosan films for the removal of food dyes from aqueous solutions by adsorption, Chem. Eng. J. 214 (2013) 8–16.
[45] J. Galán, A. Rodríguez, J.M. Gómez, S.J. Allen, G.M. Walker, Reactive dye adsorption onto a novel mesoporous carbon, Chem. Eng. J. 219 (2013) 62–68.
[46] J. Mittal, V. Thakur, A. Mittal, Batch removal of hazardous azo dye Bismark Brown R using waste material hen feather, Ecol. Eng. 60 (2013) 249–253.
[47] S.M. Al-Rashed, A.A. Al-Gaid, Kinetic and thermodynamic studies on the adsorption behavior of Rhodamine B dye on Duolite C-20 resin, J. Saudi Chem. Soc. 16 (2012) 209–215.
[48] M. Ghaedi, G. Negintaji, H. karimi, F. Marahel, Solid phase extraction and removal of brilliant green dye on zinc oxide nanoparticles loaded on activated carbon: New kinetic model and thermodynamic evaluation, J. Ind. Eng. Chem. (in press).
[49] H.N. Bhatti, Y. Safa, Removal of anionic dyes by rice milling waste from synthetic effluents: equilibrium and thermodynamic studies, Desalin. Water Treat. 48 (2012) 267–277.
[50] E. Oguz, B. Keskinler, Determination of adsorption capacity and thermodynamic parameters of the PAC used for bomaplex red CR-L dye removal, Colloids Surf. A 268 (2005) 124–130.
[51] D.L. Guerra, W.L.L. Silva, H.C.P. Oliveira, R.R. Viana, C. Airoldi, Organofunctionalized Amazon smectite for dye removal from aqueous medium—Kinetic and thermodynamic adsorption investigations, J. Hazard. Mater. 186 (2011) 675–682.
[52] V.K. Gupta, A. Mittal, D. Jhare, J. Mittal, Batch and bulk removal of hazardous colouring agent Rose Bengal by adsorption techniques using bottom ash as adsorbent, RSC Advances 2 (2012) 8381–8389.
[53] F. Geyikçi, E. Kılıç, S. Çoruh, S. Elevli, Modelling of lead adsorption from industrial sludge leachate on red mud by using RSM and ANN, Chem. Eng. J. 183 (2012) 53–59.
[54] A. Zuorro, M. Fidaleo, R. Lavecchia, Response surface methodology (RSM) analysis of photodegradation of sulfonated diazo dye Reactive Green 19 by UV/H_2O_2 process, J. Environ. Manage. 127 (2013) 28–35.
[55] A.M.M. Vargas, A.C. Martins, V.C. Almeida, Ternary adsorption of acid dyes onto activated carbon from flamboyant pods (Delonix regia): Analysis by derivative spectrophotometry and response surface methodology, Chem. Eng. J. 195–196 (2012) 173–179.
[56] E. Pajootan, M. Arami, N.M. Mahmoodi, Binary system dye removal by electrocoagulation from synthetic and real colored wastewaters, J. Taiwan Inst. Chem. E. 43 (2012) 282–290.
[57] E. Errais, J. Duplay, F. Darragi, I. M'Rabet, A. Aubert, F. Huber, G. Morvan, Efficient anionic dye adsorption on natural untreated clay: Kinetic study and thermodynamic parameters, Desalination 275 (2011) 74–81.
[58] N. Aktaş, İ.H. Boyacı, M. Mutlu, A. Tanyolaç, Optimization of lactose utilization in deproteinated whey by Kluyveromyces marxianus using response surface methodology (RSM), Bioresour. Technol. 97 (2006) 2252–2259.